



DESIGN OF SLAB-COLUMN CONNECTIONS TO RESIST SEISMIC LOADING

Simon BROWN¹, Walter DILGER²

SUMMARY

The paper presents a simple method for the punching shear design of slab column connections subjected to seismic loading. It is proposed to base the punching shear design on the probable unbalanced moment capacity of the connection, promoting a flexural failure mode over a shear failure mode. In this way a ductile failure mechanism is assured for the connection. The method does not require the calculation of the unbalanced moment caused by the lateral displacement resulting from seismic activity. This moment is difficult to calculate accurately as the analysis is highly sensitive to the effective stiffness used for the slab, column, and slab column joint.

The probable unbalanced moment capacity of the connection is primarily a flexural property. As such it can readily be approximated using the yield line procedure. The paper presents a modified yield line approach proposed by the authors. It differs most significantly from previous work in that it does not feature positive flexural yield lines. Positive yield lines are not observed in tests of slab-column connections. The internal work associated with the removal of the positive yield lines is developed in the paper and it is demonstrated that the proposed new method, without positive yield lines, results in a lower energy pattern than one with positive yield lines. The predictions of probable unbalanced moment, based on the proposed approach, are compared with results found in the literature.

INTRODUCTION

Due to their economy and speed of construction, flat slabs are very common structural elements for apartments, office and institutional buildings. It is well established, however, that the capacity of flat slabs is often governed by shear capacity in the vicinity of the columns. In addition, slabs without shear reinforcement are known to have very limited ductility under reversed cyclic loading, Brown and Dilger [1]. The collapse of several such floors during earthquakes in past years suggests that flat slabs are not suitable for zones of strong seismic activity.

Studies, Hawkins [2], have shown that properly detailed traditional stirrups substantially increase the punching resistance of a slab-column connection subjected to combined punching load and unbalanced moment. More recent studies, Dilger and Ghali [3], show that shear studs are a more effective means of

¹ Project Engineer, Read Jones Christoffersen Ltd., Calgary, Canada. Email: sbrown@rjc.ca

² Professor Emeritus, University of Calgary, Calgary, Canada. Email: dilger@ucalgary.ca

enhancing shear strength than traditional stirrups. There is also a growing body of evidence, Cao [4], Dilger and Cao [5], Megalli [6], and Dilger and Brown [7], that shear studs are also highly effective in increasing both the connection capacity under reversed cyclic loading as well as ductility. Shear studs have the added advantage that they are much easier to install than traditional stirrups.

Given the above, it is then of interest to develop design guidelines for the use of flat slab column connections in seismic zones. These connections may be considered to act in one of two capacities during seismic loading. In the first case, the slab column system acts as a moment resisting frame. This frame action then provides the primary lateral load resisting mechanism of the structure. This type of system will be the subject of a future paper and will not be discussed further here. In the second scenario, an independent lateral load resisting mechanism, such as shear walls, is provided in the building. In this case, the slab column connections need only continue to carry the gravity load tributary to them while undergoing the rotations associated with the displacements imposed by the primary system. It is the design requirements for connections in building with this type of system that are the subject of this paper.

The design of a slab column connection in this second case is relatively strait forward once the magnitude of the unbalanced moment resulting from the lateral drift of the structure is determined. The primary complication that arises is that it is somewhat difficult to determine this moment with accuracy. This is due to the fact that the unbalanced moment calculated for a given inter-story drift is highly dependent on the assumptions made regarding the relative stiffness' of the slab and column elements. This is further complicated by the fact that as inter-story drift ratios become greater, the relationship between drift and unbalanced moment becomes less than linear due to yielding of the flexural reinforcement.

One way to overcome these problems is to calculate the maximum unbalanced moment capacity of the connection based solely on the flexural limitations of the slab in the vicinity of the column. If the punching shear design is then completed such that this maximum unbalanced moment can be resisted, in combination with the anticipated gravity load at the time of an earthquake, a ductile flexural failure mechanism can be ensured. This is consistent with the "Capacity Design" approach proposed by Park and Pauly [8] where plastic hinge locations are consciously selected and appropriately detailed. This paper is primarily concerned with the derivation of a method that can be used to determine the peak unbalanced moment capacity of a given connection.

PEAK UNBALANCED MOMENT CAPACITY OF A SLAB COLUMN CONNECTION

Perhaps the most convenient way to determine the probable maximum unbalanced moment capacity of a connection, M_{pr} , is by way of a yield line approach. This approach has been used before and the pattern presented here is not an entirely new creation but is based on patterns proposed by Dilger and Cao [9] as well as Gesund [10] before them. The derivation that follows was part of a dissertation completed at the University of Calgary, Brown [11], and builds on the work of these authors. The pattern developed here is intended to be applicable to "typical" loading conditions. Load cases near the extremes of pure concentric load or pure unbalanced load are outside the intended scope of this procedure.

Figure 1 shows the pattern of flexural failure proposed by Dilger and Cao. This pattern consists of radial negative yield lines about the column bounded by a roughly oval positive yield line. Using this pattern, the following relation can be derived:

$$M_{pr} = 2(1 + \pi)(1 + k)mc - 0.5Vc \quad [1]$$

where:

- m negative flexural moment capacity per unit width
- c dimension of square column

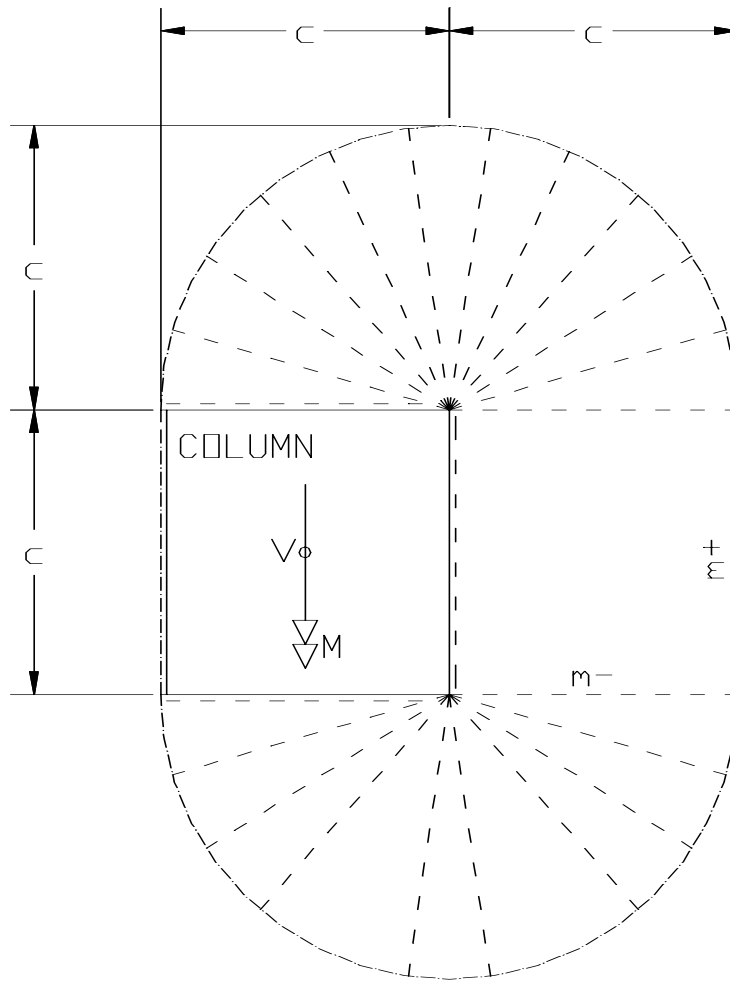


Figure 1 - Yield Line Pattern As proposed by Cao and Dilger

- k ratio for positive to negative flexural capacity of slab per unit width
 V Total vertical load applied by slab to column

This equation produces reasonably good results in comparison with test results. Further, the crack pattern that can be observed on the top surface of test specimens is similar to the assumed negative yield line pattern. Laboratory tests, however, do not exhibit the positive flexural cracking implicit in the derivation. In addition, Eqn. 1 requires extension to the more general condition of rectangular columns and non-orthotropic flexural reinforcing.

To further examine this, as well as to expand the equation to the more general case, the radial yield line portion of the pattern is examined in more detail, see Fig. 2. The figure represents a quarter circular section of the slab, of radius R , deflected up “unity” at the central corner.

Internal Energy associated with Radial Negative Yield Lines

Considering only the radial negative yield lines, it can be shown that the total internal energy, $U_{quarters}$, required to displace the corner of the section of slab up “unity” can be expressed as:

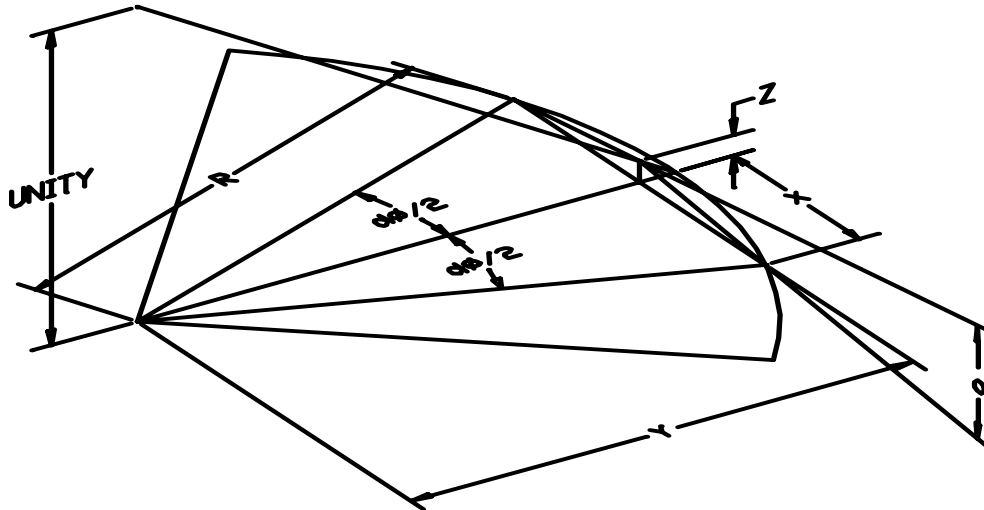


Figure 2 - Geometry of Negative Yield Line 'Fan'

$$U_{quarter} = \frac{2m\pi \left(1 - \cos\left(\frac{d\phi}{2}\right)\right)}{d\phi \sin\left(\frac{d\phi}{2}\right)} \quad [2]$$

The internal energy dissipated is not a function of the radius, R , of the fan pattern assumed. This is sufficient, in itself, to explain why positive yield lines do not form and are not observed in the laboratory. The negative yield lines can extend indefinitely without an increase in the internal energy. The formation of positive yield lines would require additional energy input. They are therefore precluded from forming. As the angle between adjacent negative yield lines, $d\phi/2$, approaches zero the internal energy, $U_{quarter}$, approaches a value of:

$$U_{quarter} = \frac{\pi m}{2} \quad [3]$$

Internal Energy associated with Perimeter of Yield Line Pattern

In the yield line pattern shown in Fig. 2, a geometric discontinuity is represented at the circular boundary of the negative yield lines. Previous researchers have addressed this discontinuity by introducing a positive yield line. A result of this extra yield line, however, is that the internal energy associated with the pattern is increased. As noted above, the length of the negative yield lines can increase without a corresponding increase in the associated internal energy of the pattern. Therefore, in an infinite slab the geometric discontinuity can be removed by allowing the length of the yield lines to extend indefinitely. Despite the infinite extend of the resulting pattern, this produces in a lower energy solution than is achieved by introducing a bounding positive yield line.

Infinite slabs are, however, generally not practical to construct and so the more general finite case must be considered. In addition, a slab under gravity load is not initially planar. These conditions not only effect the maximum length of yield line that can be assumed, but also introduce additional internal energy mechanisms at the boundary of the yield line pattern. Of great significance is that, as a result of the fact

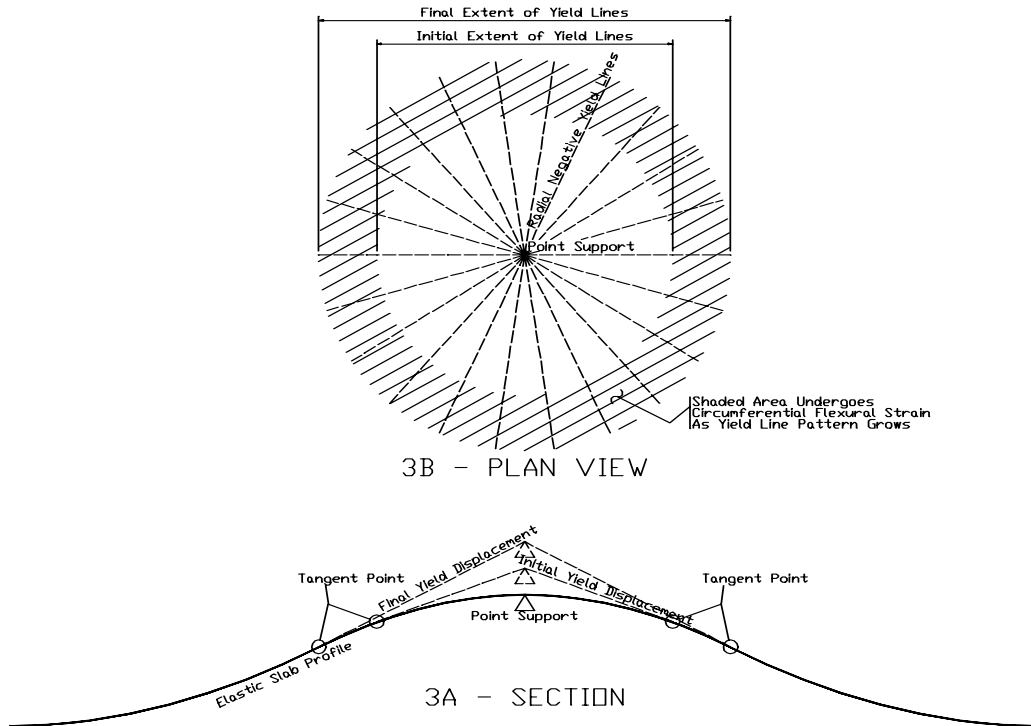


Figure 3 - Yield Line Development for Point Load

that slabs under gravity load are not initially planar, the length of the radial negative yield lines must increase as the displacement is increased.

This is illustrated in Fig. 3A. The figure represents, conceptually, the profile of a slab that was initially planar with no load on it. As gravity load is introduced the elastic deflected shape indicated by the heavy line results. At some point the flexural capacity at the support of the slab is exceeded and a local flexural failure, the start of a yield line pattern, develops at the support. The dashed line in the figure represents this. In the figure, the support is represented as displacing up for clarity. In reality the support would remain stationary and the slab would deflect down.

In the case of concentric point loading the yield line pattern would consist of radial negative yield lines arranged over 360° around the load. This pattern produces a cone shaped deflection at the support, see Fig. 3B. Note that, as the yield line cone is tangent to the elastic portion of the slab, there is no geometric discontinuity at the perimeter of the pattern and therefore no requirement for a positive yield line. As the load increases further, and assuming the positive flexural capacity of the slab at mid-span is not exceeded, the slab displaces further and the size of the yield line cone increases, see the upper dashed line in Fig. 3A.

The internal work associated with the rotation of the radial negative yield lines resulting from this displacement can be calculated using Eqn. 3. In addition to the work related to moments in the radial direction, however, work is also done by moments in the circumferential direction in the portion of the slab between the two cones that has been 'strained out', see the shaded portion of Fig. 3B.

As the shaded portion of the slab in Fig. 3B is strained out in the circumferential direction, ignoring the influence of tangential flexural strains on circumferential moments, the moment reduces linearly from its

initial value to zero. For a small increase in displacement, for which it can be assumed that the initial moment m_{circ} and the applied flexural strain K_{circ} in the shaded area, A_{circ} , is roughly uniform, the associated internal energy, U_{circ} , can be shown to be:

$$U_{circ} = \int_{Area} \left[\frac{1}{2} m_{circ} K_{circ} \right] da = \frac{1}{2} m_{circ} K_{circ} A_{circ} \quad [4]$$

It is important to note that as the direction of circumferential moment, m_{circ} , is acting in an opposite sense to the direction of the applied flexural strain, K_{circ} , the associated internal energy, U_{circ} , is negative. This means that the circumferential moments are actually driving the development of the yield line pattern. As the size of the yield line pattern grows, the magnitudes of both m_{circ} , and K_{circ} , become smaller and smaller. Both become zero as the radial negative yield lines approach the inflection point of the slab. As a result the energy associated with the circumferential yield lines, U_{circ} , also becomes zero as the yield line pattern extends to the inflection point of the slab.

The significance of the above is that the load associated with the yield line pattern increases as the size of the yield line pattern becomes larger. A maximum value is reached as the negative radial yield lines reach the inflection point of the slab. At this point the value of U_{circ} is zero. This means that when considering the loads associated with the proposed yield line, the influence of the circumferential moments can be ignored. It also suggests that the yield line pattern should be assumed to extend to the inflection point of the slab.

Variation of Shape and Non-Orthotropic Reinforcement

It was assumed above that the yield line pattern was circular. It is worth considering the influence of an elliptical, as opposed to circular, pattern. It is intuitively obvious that the circular case should produce either a local maxima or local minima. If one of the straight edges of the quarter circular section shown in Fig. 2 is assumed slightly longer than the other, the resulting internal energy is expected to differ somewhat from that for the circular case. It is, however, not expected that it would matter which of the edges was the longer one. It can, in fact, be shown that when the ratio of the length of one edge to the other is n , the resulting internal energy associated with a unit displacement at the corner can be expressed as:

$$U = \frac{(1+n^2)}{2n} U_{circular} = \frac{(1+n^2)\pi m}{4n} \quad [5]$$

It is clear from the above that the circular section governs over the elliptical. That is, the minimum value of U is obtained by setting $n = 1.0$. This is, however, true only when the moment resistance, per unit width of slab, is the same in each of the two orthogonal directions. In the event that the negative moment capacities, m_x and m_y , are not the same, it can be shown by using the method of affine slabs, Ghali & Neville [12], that:

$$U_{quarter} = \frac{\pi}{2} \sqrt{m_y m_x} \quad [6]$$

Where m_x does not equal m_y , an elliptical yield line pattern produces the minimum energy pattern. The ratio of the side lengths, n , can then be expressed:

$$n = \sqrt{\frac{m_y}{m_x}} \quad [7]$$

Geometry of a Yield Line Pattern for an Interior Column with Unbalanced Moment

The above derivation of a yield line pattern for a slab on point supports can now be extended to the case of an interior rectangular column with unbalanced moment. The general geometry of the pattern is as indicated in Fig. 4. The pattern is characterized by two semicircular ‘fans’ of radial negative yield lines

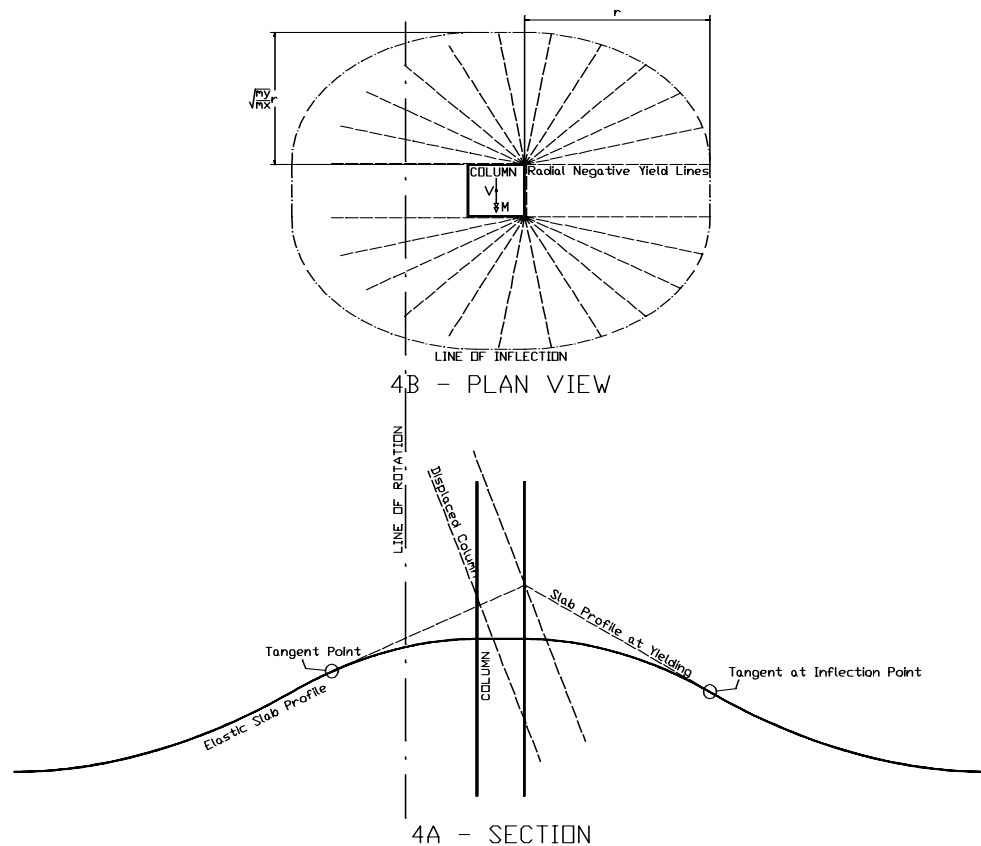


Figure 4 - Yield Line Development for Interior Column

centered on the forward corners of the column. The slab at these corners is ‘pushed up’ by the rotation of the column in a manner similar to the point support in Fig. 3. The slab then forms half cones sloping away from these corners. As with the previous example the supports do not really displace up, rather the slab displaces down.

On the forward side of the column, the yield lines extend to the inflection point in the slab, see Fig. 4A and 4B. As previously discussed this condition is anticipated to coincide with the peak unbalanced moment. If the internal energy of the pattern is to be minimized, Eqn. 7 must govern the width. This is shown coinciding with the inflection point in the slab, see Fig 4B. In general this will not be the case. In fact, if the cone is to intercept the elastic slab profile on a tangent, neither of these conditions may be satisfied. Although this will have some effect on the internal energy associated with the pattern, for typical slab layouts, the error introduced by ignoring this is small. As a result, this effect is not considered further here.

On the backside of the column, the cone will again extend tangent to the elastic slab profile. Again, this eliminates the need for a positive yield line on the backside. In general, however, due to the length of the column, this will not coincide with the inflection point of the slab. This results in the two separate effects on the internal energy calculations. Firstly, as the pattern does not extend to the inflection point, the internal energy is reduced due to the influence of U_{circ} , Eqn. 4. This is countered somewhat, however, by an increase in internal energy resulting from the fact that the aspect ratio of the back quarter ‘fan’ patterns is not optimized, Eqn. 5. This effect varies primarily as a function of the length of the column, measured

in the direction of seismic activity, relative to the free span of the slab. For column dimensions less than 20% of the free span of the slab the effect of this on the internal energy associated with the pattern is less than approximately 10%. This is again neglected in the derivation that follows.

Of greater influence on the derivation is location of the line of rotation, see Fig. 4. The distance between this and the center of the column has a direct influence on how large a roll the concentric gravity load will have on the resistance of the connection to unbalanced moment. The actual location of this line is not fixed during loading and, in addition, varies as a function of the column size measured in the direction of seismic loading, as well as the magnitude of the gravity load being transferred to the column by the slab. It is proposed here to use the intersection of the initial plane of the slab at the column and the final profile of the backside yield line as the effective centre of rotation, see Fig. 4B.

As noted previously, the magnitude of the concentric shear force can have a significant influence on the yield line pattern that develops at the columns. For very highly loaded connections, a yield line pattern, similar to that shown in Fig. 3, can develop prior to the application of unbalanced moment. For connections where there is very little gravity load, the elastic profile indicated in Fig. 4 may not provide sufficient rotation capacity on the backside of the column. In this case positive yield lines would be required. For a slab detailed to current North American design codes, however, it is reasonable to assume that, under specified dead load only, the top bars at the face of the column will be close to, or just beyond, yield strain. This is the condition assumed here. The fully developed elastic slab profile required to eliminate the development of positive yield lines is assumed to be available, but without any significant pre-existing yielding of the top bars. Given this, the center of rotation will always start at the back face of the column and move further back, toward the back inflection point, as column rotation increases.

The larger the column dimension in the direction of seismic activity, the further the centre of rotation is from the center of the column at the start of seismic loading. In addition, however, the larger the column dimension, the less the center of rotation moves back into the slab as column rotation increases. Although these effects counter each other somewhat, varying the column dimension does have a significant influence on the determination of the centre of rotation as defined above. For column dimensions, measured in the direction of seismic loading, between 0.05 and 0.1 of the clear span the distance between the centre of rotation and the forward corners of the column, the apex of the displaced cones, varies from 2.5 to 1.5 times the column dimension. In order to reduce the number of variables in the derived equations, the centre of rotation is assumed fixed at a location twice the column dimension behind the forward face of the column, $2 c_y$.

Equations of Energy for Interior Yield Line Pattern Moment

In this section, the internal energy and external work equations are developed for the yield line pattern shown in Fig. 4. The equations are all presented for a unit rotation of the column about the line of rotation, see Fig. 4A. For a unit rotation of the slab, the forward corners of are displaced vertically a distance:

$$\delta = \frac{2 c_y}{2} = c_y \quad [8]$$

where c_y is the dimension of the column in the direction of seismic loading. The value of 2 in the denominator of Eqn. 8 represents that fact that half of the total change in height of the cone is associated with the downward movement of the outer perimeter of the cone. As this is assumed to be tangent to the elastic profile, no internal work is associated with this half of the displacement. The energy associated with the radial yield lines, U_{radial} , is then:

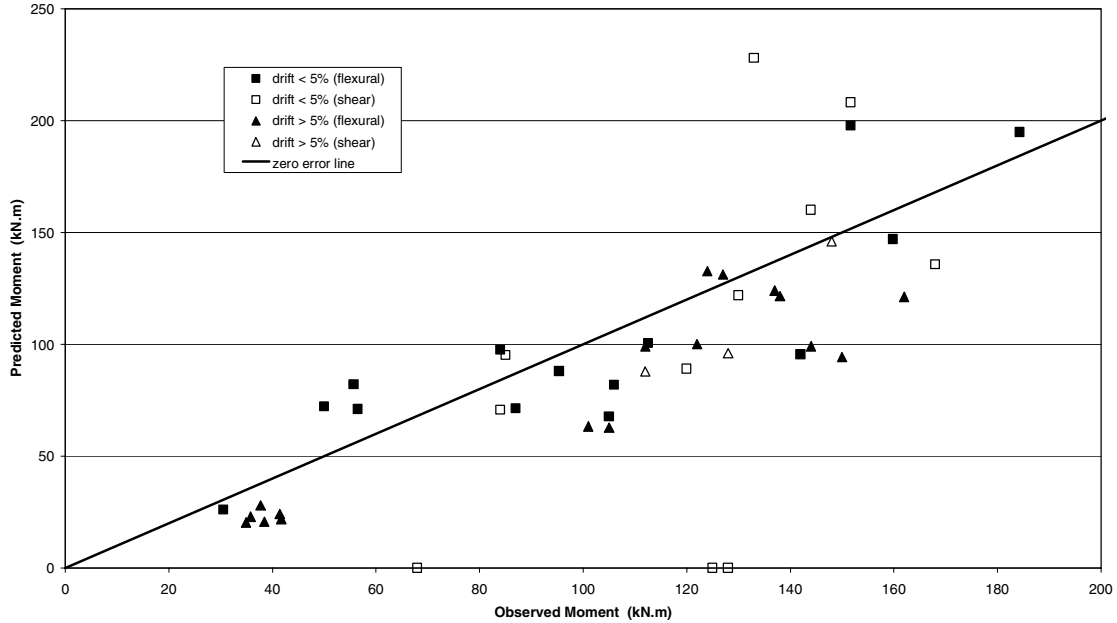


Figure 5 - Comparison of Predicted and Observed Unbalanced Moments

$$U_{radial} = 4 \delta U_{quarter} = 4 c_y \frac{\pi \sqrt{m_y m_x}}{2} = 2 \pi c_y \sqrt{m_y m_x} \quad [9]$$

In addition to this the internal energy associated with the negative yield line at the front face of the column must be added. This yield line undergoes a rotation of slightly less than twice the rotation of the column. The total internal energy, U , associated with the yield line pattern is then:

$$U = 2 \pi c_y \sqrt{m_y m_x} + 2 c_x m_x \quad [10]$$

Where c_x is the dimension of the column perpendicular to the direction of seismic activity. The work done by the external loads, W , as the column rotates about the slab can be determined as:

$$W = M + \left(\frac{3 c_y}{4} \right) V \quad [11]$$

Equating Eqn. 10 and 11 and solving for the unbalanced moment, M :

$$M = 2 \pi c_y \sqrt{m_y m_x} + 2 c_x m_x - \frac{3 c_y}{4} V \quad [12]$$

COMPARISON OF PREDICTED UNBALANCED MOMENT CAPACITY WITH EXPERIMENTAL RESULTS

Figure 5 and Table 1 show the correlation between the predicted unbalanced moments, using the above derivation, compared with actual test results. In general the predicted results agree very well with test result. The mean error is only about 1% while the standard deviation of the absolute error is 19%.

In some of the tests reported in Table 1 the predicted unbalanced moment capacity is significantly greater than the observed capacity, most notably Cao and Dilger specimen CD-1. This is due to the fact that this specimen, which was subjected to a very high concentric load of 300 kN, did not contain any shear reinforcement. As a result it failed in punching shear prior to reaching its full flexural capacity.

Table 1 - Summary of Available test data

| Researchers | Original Designation | loading | cx mm | cy mm | davg mm | rhot | fy MPa | fc MPa | V kN | m neg kN.m/m | m pos kN.m/m | Mtest kN.m | Mpr kN.m | Error |
|----------------|----------------------|-------------|-------------|----------|------------|--------|-----------|-----------|---------|-----------------|-----------------|---------------|-------------|--------|
| Hawkins et al. | S2 | rev. cyclic | 305 | 305 | 117 | 0.0084 | 464 | 23 | 143 | 48 | 29 | 95 | 88 | -7.7% |
| | S4 | rev. cyclic | 305 | 305 | 117 | 0.0120 | 460 | 32 | 150 | 67 | 35 | 168 | 136 | -19.2% |
| Hawkins et al | SS1 | rev. cyclic | 305 | 305 | 117 | 0.0129 | 460 | 28 | 133 | 70 | 35 | 160 | 147 | -8.0% |
| | SS2 | rev. cyclic | 305 | 305 | 117 | 0.0090 | 464 | 26 | 127 | 51 | 29 | 113 | 101 | -10.6% |
| | SS3 | rev. cyclic | 305 | 305 | 117 | 0.0176 | 456 | 26 | 127 | 89 | 51 | 184 | 195 | 5.7% |
| | SS4 | rev. cyclic | 305 | 305 | 117 | 0.0176 | 456 | 28 | 128 | 90 | 51 | 152 | 198 | 30.4% |
| | SS5 | rev. cyclic | 305 | 305 | 117 | 0.0176 | 464 | 32 | 126 | 94 | 53 | 152 | 208 | 37.2% |
| Elmasri et al | SM 0.5 | monotonic | 305 | 305 | 127 | 0.0050 | 475 | 37 | 129 | 37 | 12 | 101 | 63 | -37.3% |
| | SM 1.0 | monotonic | 305 | 305 | 127 | 0.0100 | 475 | 33 | 129 | 70 | 25 | 128 | 147 | 14.6% |
| | SM 1.5 | monotonic | 305 | 305 | 127 | 0.0150 | 475 | 40 | 129 | 102 | 37 | 133 | 228 | 71.4% |
| | SM 0.5/0.5 | monotonic | 305 | 305 | 127 | 0.0050 | 475 | 33 | 129 | 37 | 12 | 105 | 63 | -40.2% |
| | SM 1.0/2.0 | monotonic | 305 | 305 | 127 | 0.0100 | 475 | 32 | 129 | 70 | 25 | 148 | 146 | -1.3% |
| | SM 1.5/2.0 | monotonic | 305 | 305 | 127 | 0.0150 | 475 | 34 | 401 | 100 | 37 | 144 | 160 | 11.2% |
| Pan and Moehle | AP1 | rev. cyclic | 274 | 274 | 103 | 0.0086 | 485 | 29 | 104 | 41 | 15 | 57 | 71 | 25.7% |
| | AP2 | rev. cyclic | 274 | 274 | 103 | 0.0086 | 485 | 30 | 104 | 41 | 15 | 87 | 71 | -18.1% |
| | AP3 | rev. cyclic | 274 | 274 | 103 | 0.0086 | 485 | 32 | 53 | 41 | 15 | 56 | 82 | 47.3% |
| | AP4 | rev. cyclic | 274 | 274 | 103 | 0.0086 | 485 | 31 | 53 | 41 | 15 | 106 | 82 | -22.8% |
| Islam and Park | 1 | monotonic | 229 | 229 | 70 | 0.0106 | 356 | 27 | 34 | 17 | 9 | 31 | 26 | -14.6% |
| | 2 | monotonic | 229 | 229 | 70 | 0.0106 | 374 | 32 | 34 | 18 | 9 | 38 | 28 | -25.8% |
| | 3C | rev. cyclic | 229 | 229 | 70 | 0.0106 | 316 | 30 | 34 | 15 | 8 | 36 | 23 | -35.9% |
| | 4S | monotonic | 229 | 229 | 70 | 0.0106 | 329 | 32 | 34 | 16 | 8 | 41 | 24 | -41.6% |
| | 6CS | rev. cyclic | 229 | 229 | 70 | 0.0106 | 290 | 28 | 34 | 14 | 7 | 38 | 21 | -46.2% |
| | 7CS | rev. cyclic | 229 | 229 | 70 | 0.0106 | 304 | 30 | 34 | 15 | 8 | 42 | 22 | -47.4% |
| | 8CS | rev. cyclic | 229 | 229 | 70 | 0.0106 | 293 | 22 | 34 | 14 | 7 | 35 | 20 | -41.6% |
| | Brown and Dilger | SJB-1 | rev. cyclic | 250 | 250 | 115 | 0.0129 | 400 | 32 | 150 | 61 | 23 | 112 | 99 |
| SJB-2 | | rev. cyclic | 250 | 250 | 115 | 0.0154 | 400 | 34 | 150 | 72 | 23 | 138 | 122 | -11.9% |
| SJB-3 | | rev. cyclic | 250 | 250 | 115 | 0.0129 | 400 | 32 | 150 | 61 | 23 | 144 | 99 | -31.1% |
| SJB-4 | | rev. cyclic | 250 | 250 | 115 | 0.0154 | 400 | 40 | 150 | 73 | 23 | 137 | 124 | -9.5% |
| SJB-5 | | rev. cyclic | 250 | 250 | 115 | 0.0168 | 400 | 33 | 150 | 78 | 23 | 124 | 133 | 7.1% |
| SJB-6 | | monotonic | 250 | 250 | 115 | 0.0129 | 400 | 36 | 150 | 62 | 23 | 125 | 100 | -19.7% |
| SJB-7 | | rev. cyclic | 250 | 250 | 115 | 0.0129 | 400 | 29 | 150 | 61 | 23 | 84 | 97 | 16.1% |
| SJB-8 | | rev. cyclic | 250 | 250 | 115 | 0.0129 | 400 | 35 | 150 | 62 | 23 | 122 | 100 | -17.9% |
| SJB-9 | | rev. cyclic | 250 | 250 | 115 | 0.0168 | 400 | 31 | 150 | 77 | 23 | 127 | 131 | 3.3% |
| Cao and Dilger | CD-1 | rev. cyclic | 250 | 250 | 115 | 0.0129 | 395 | 40 | 300 | 62 | 24 | 50 | 72 | 44.3% |
| | CD-3 | rev. cyclic | 250 | 250 | 115 | 0.0129 | 395 | 36 | 300 | 61 | 24 | 84 | 71 | -15.8% |
| | CD-4 | rev. cyclic | 250 | 250 | 115 | 0.0129 | 395 | 34 | 200 | 61 | 24 | 120 | 89 | -25.8% |
| | CD-5 | rev. cyclic | 250 | 250 | 115 | 0.0129 | 395 | 31 | 200 | 61 | 24 | 68 | 88 | 29.2% |
| | CD-6 | rev. cyclic | 250 | 250 | 115 | 0.0129 | 395 | 31 | 200 | 61 | 24 | 112 | 88 | -21.5% |
| | CD-7 | rev. cyclic | 250 | 250 | 115 | 0.0129 | 395 | 29 | 150 | 60 | 23 | 128 | 96 | -25.0% |
| | CD-8 | rev. cyclic | 250 | 250 | 115 | 0.0129 | 395 | 27 | 150 | 60 | 23 | 85 | 95 | 11.9% |
| | Elgabry and Ghali | 1 | monotonic | 250 | 250 | 117 | 0.0131 | 452 | 35 | 150 | 72 | 28 | 130 | 122 |
| 2 | | monotonic | 250 | 250 | 117 | 0.0131 | 452 | 34 | 150 | 72 | 28 | 162 | 121 | -25.1% |
| 3 | | monotonic | 250 | 250 | 117 | 0.0131 | 452 | 39 | 300 | 73 | 28 | 142 | 96 | -32.7% |
| 4 | | monotonic | 250 | 250 | 117 | 0.0131 | 446 | 41 | 300 | 73 | 28 | 150 | 94 | -37.1% |
| 5 | | monotonic | 250 | 250 | 117 | 0.0131 | 446 | 46 | 450 | 73 | 28 | 105 | 68 | -35.6% |

Ref. [4], [11], [13], [14], [15], [16], and [17]

In Fig. 5, the specimens that, according to Canadian design code CSA-A23.3, would be expected to fail in shear prior to reaching the predicted unbalanced moments are indicated with open markers. In addition, the specimens that did not fail until the drift ratio was greater than 5% are indicated with triangular markers. It is reasonable to assume that these specimens reached their maximum unbalanced moment capacities.

It is seen in Fig. 5 that the proposed equation gave best results for specimens that were able to resist 5% column rotations or greater, triangular markers. These are the specimens that the proposed method is expected to correlate best with. Where the specimens were not able to undergo an inter-storey drift ratio of at least 5%, square markers, the proposed method resulted in a somewhat greater scatter of results. In general, however, the predictions were better where pre-mature shear failure was not predicted to govern the results.

ADDITIONAL CONSIDERATIONS

In the previous section, a method of predicting the probable unbalanced moment that a slab column connection can be expected to resist, based on flexural failure, was presented. In this section additional factors that should be considered when designing for punching shear under seismic conditions will be presented. Generally the design for punching under seismic loading is identical to that under gravity loading. Three additional recommended practices have, however, also been identified, Brown [11].

The first of these relates to the shear stress that can be assumed to be resisted by the concrete, v_c , in the presence of shear reinforcement. Under seismic loading, the shear resistance of the concrete is less than under static loading. It is then recommended that, for seismic design, the value of v_c be taken as half the value permitted by code for gravity loading. In addition to this, it is also reasonable to specify a minimum level of shear reinforcement, once the use of reinforcement is mandated. It is proposed by Brown [11] to provide a minimum of $v_s = 0.15\sqrt{f'_c}$ if headed studs are used and $v_s = 0.20\sqrt{f'_c}$ if traditional stirrups are used. These are minimum values that may need to be increased for greater load requirements. Finally, some thought needs to be given to the extent of the shear reinforced zone from the face of the column. For static loading, North American design codes specify a minimum extension of $2d$ from the face of the column, where d is the effective depth of the slab. It is proposed here to double this in the case of seismic loading to $4d$.

One final point worth consideration is to provide some guidance as to when design for seismic considerations needs to be done. Where seismic displacements are small, and/or the concentric gravity load is light, special detailing for seismic loading may not be required. The head of the seismic sub-committee to CSA A23.3, Mr. Mutrie, proposed a suitable equation. His review of available data, derived largely from test results reported by Megally [18], indicated that, for slabs without shear reinforcement, there exists a relationship between the ratio v_f/v_r , in non-shear-reinforced connections, and the amplitude of reverse cyclic drift that can be applied without failure. The relation is expressed as:

$$\frac{v_f}{v_r} \leq R_E = \left(\frac{0.005}{\Delta_i} \right)^{0.85} \leq 1.0 \quad [13]$$

In Eqn. 13, Δ_i is the maximum inter-storey drift anticipated to occur during seismic activity. The term v_f is the factored shear stress on the critical section and v_r is the factored shear stress resistance at that section. Equation 13 is intended to be used for connections that do not contain shear reinforcement. As a result, v_r is equal to the shear stress resistance of the concrete acting alone, v_c .

This equation provides a convenient benchmark to determine if additional attention is required as to the seismic resistance of the connection. Provided the ratio of v_f , calculated for seismic load combinations, to v_r , is less than R_E , calculated for the anticipated level of inter-storey drift, it is sufficient to detail the connections for gravity load only.

SUMMARY

The economy of flat slab construction, from the point of view of forming requirements, combined with their open and unobstructed soffit layout have made them a very popular structural forms, particularly in the high-rise condominium market where floor to floor heights are kept to a minimum. This popularity, combined with the fact that most major cities in North America are now seismically zoned to some degree,

makes the lack of adequate code guidance on the detailing of these connections to resist earthquake induced loads a very serious concern.

What is required is a simple method to design the punching shear resistance of a slab column connection subjected to seismically induced displacements. The connection must be able to continue to resist the gravity loads tributary to it, while undergoing the reversed cyclic rotations of the column about its connection to the slab that are induced during seismic activity. The primary difficulty is in determining the unbalanced moment, transferred between the slab and the supporting columns, associated with seismic loading.

This paper has presented a simplified method for determining the peak unbalanced moment capacity of a slab column connection based on flexural limitations. This value can conservatively be used as the unbalanced moment for punching shear design to ensure that a brittle shear type failure is avoided. The proposed method has been compared with laboratory results found in the literature and appears to give reasonable results. Some additional design considerations specific to the punching shear design of slabs for seismic resistance have also been given.

REFERENCES

1. Brown, S., Dilger, W. H. "Seismic Response of Flat Plate Column Connections", Proc. CSCE, Winnipeg, Manitoba, Canada, 1994.
2. Hawkins, N.M. "Shear Strength Of Slabs With Shear Reinforcement," Shear in Reinforced Concrete, ACI Special Publication SP-42, Detroit, 1974, pp. 785-816.
3. Dilger, W. H., Ghali, A. "Shear Reinforcement for Concrete Slabs", Proc. ASCE, Proc. Vol. 107, No. ST12, 1981, pp. 2403-2420.
4. Cao, H. "Seismic Design of Slab-Column Connections", M.Sc. Thesis, The University of Calgary, 1993.
5. Dilger, W. H., Cao, H. "Behavior of Slab-Column Connections Under Reversed Cyclic Loading", Proc. 5th International Colloquium on Concrete, Cairo, Egypt, 1994, pp. 595-606.
6. Megally S.H., "Punching Shear Resistance of Concrete Slabs to Gravity and Earthquake Forces", Ph.D. Thesis, University of Calgary, Calgary, 1998.
7. Dilger W. H., Brown S. J., "Earthquake Resistant Slab-Column Connections", Festschrift Prof. Dr. Hugo Bachman Zum 60, Geburtstag, Institut für Baustatik und Konstruktion, ETH Zürich, Sept. 1995, pp. 22-27.
8. Park R., Pauly T., "Reinforced Concrete Structures", John Wiley & Sons, Sydney, 1975.
9. Dilger, W. H., Cao, H. "Behavior of Slab-Column Connections Under Reversed Cyclic Loading", Proc. 5th International Colloquium on Concrete, Cairo, Egypt, 1994, pp. 595-606.
10. Gesund H. "Design for Punching Strength of Slabs at Interior Columns", Advances in Concrete Technology, Dergamon Press, Proc. International Conference on Concrete Slabs Held at Dundee University, 3 – 6 April, 1980, Great Britain, 1980, pp. 173-184.

11. Brown, S. "Seismic Response of Slab-Column Connections", Ph.D. Dissertation, The University of Calgary, 2003.
12. Ghali A., Neville A. M., "Structural Analysis – A Unified Classical and Matrix Approach" Third Edition, Chapman and Hall., New York, 1989.
13. Hawkins, N. M., Mitchell, D., Hanna, S. H. "The Effect Of Shear Reinforcement On The Reversed Cyclic Loading Behavior Of Flat Plate Structures", Canadian Journal of Civil Engineering, Vol. 2, 1975, pp. 572-582.
14. Elmasri M. Z., Dilger W. H., Ghali A. "Static and Dynamic Response of Slab-Column Connections to Shear and Moment", Research Report No. CE75-10, University of Calgary, November 1975, 78 pp.
15. Pan A., Moehle J. P. "Lateral Displacement Ductility of Reinforced Concrete Flat Plates", ACI Structural Journal, May - June 1989, pp 250 - 258.
16. Islam S., Park R. "Tests on Slab Column Connections with Shear and Unbalanced Flexure", ASCE, Journal of the Structural Division, Vol. 102, No. ST3, March, 1976, pp. 549 - 568.
17. Elgabry A., Ghali A. "Tests on Concrete Slab-Column Connections with Stud-Shear Reinforcement Subjected to Shear-Moment Transfer", ACI Structural Journal, Sept - Oct, 1987, pp. 433 - 442.
18. Megally S.H., "Punching Shear Resistance of Concrete Slabs to Gravity and Earthquake Forces", PhD. Thesis, University of Calgary, Calgary, 1998.